

# ESCRT-I Core and ESCRT-II GLUE Domain Structures Reveal Role for GLUE in Linking to ESCRT-I and Membranes

Hsiangling Teo,<sup>1,4,\*</sup> David J. Gill,<sup>1,4</sup> Ji Sun,<sup>3</sup> Olga Perisic,<sup>1</sup> Dmitry B. Veprintsev,<sup>2</sup> Yvonne Vallis,<sup>1</sup> Scott D. Emr,<sup>3</sup> and Roger L. Williams<sup>1,\*</sup>

<sup>1</sup>MRC Laboratory of Molecular Biology

<sup>2</sup>Centre for Protein Engineering

Medical Research Council Centre, Cambridge, CB2 2QH, United Kingdom

<sup>3</sup>Department of Cellular and Molecular Medicine, The Howard Hughes Medical Institute, University of California, San Diego, School of Medicine, La Jolla, CA 92093, USA

<sup>4</sup>These authors contributed equally to this work.

\*Contact: hlt@mrc-lmb.cam.ac.uk (H.T.); rlw@mrc-lmb.cam.ac.uk (R.L.W.)

DOI 10.1016/j.cell.2006.01.047

## SUMMARY

ESCRT complexes form the main machinery driving protein sorting from endosomes to lysosomes. Currently, the picture regarding assembly of ESCRTs on endosomes is incomplete. The structure of the conserved heterotrimeric ESCRT-I core presented here shows a fan-like arrangement of three helical hairpins, each corresponding to a different subunit. Vps23/Tsg101 is the central hairpin sandwiched between the other subunits, explaining the critical role of its “steadiness box” in the stability of ESCRT-I. We show that yeast ESCRT-I links directly to ESCRT-II, through a tight interaction of Vps28 (ESCRT-I) with the yeast-specific zinc-finger insertion within the GLUE domain of Vps36 (ESCRT-II). The crystal structure of the GLUE domain missing this insertion reveals it is a split PH domain, with a noncanonical lipid binding pocket that binds PtdIns3P. The simultaneous and reinforcing interactions of ESCRT-II GLUE domain with membranes, ESCRT-I, and ubiquitin are critical for ubiquitinated cargo progression from early to late endosomes.

## INTRODUCTION

The multivesicular body (MVB) protein-sorting pathway targets transmembrane proteins either for degradation or for function in the vacuole/lysosomes. The signal for entry into this pathway is monoubiquitination of protein cargo, which results in incorporation of cargo into luminal vesicles at late endosomes (for reviews see, Katzmann et al., 2002; Raiborg et al., 2003). Genetic studies in yeast

have identified a group of genes that are crucial for this process and when mutated result in enlarged endosomes (Odorizzi et al., 1998; Raymond et al., 1992). A subset of these genes encodes multisubunit endosomal sorting complexes required for transport (ESCRTs), which act sequentially on endosomal membranes (reviewed in Bowers and Stevens, 2005; Hurley and Emr, 2006).

Yeast ESCRT-I consists of three protein subunits, Vps23, Vps28, and Vps37 (Babst et al., 2000; Katzmann et al., 2001). In humans, ESCRT-I comprises Tsg101, Vps28, and one of four potential human Vps37 homologs (Bache et al., 2004; Bishop and Woodman, 2001; Eastman et al., 2005; Stuchell et al., 2004). ESCRT-I is recruited to endosomes by an interaction with the Vps27/Hse1p complex (or Hrs/STAM in human), and this recruitment is required for downstream cargo sorting (Bache et al., 2003a, 2003b; Bilodeau et al., 2003; Katzmann et al., 2003; Pornillos et al., 2003). The main role of ESCRT-I is to recognize ubiquitinated cargo via the UEV domain of the Vps23/Tsg101 subunit (Bilodeau et al., 2003; Katzmann et al., 2001; Martin-Serrano et al., 2003b; Sundquist et al., 2004; Teo et al., 2004b). A C-terminal “steadiness box” within Vps23/Tsg101 has been reported to tightly regulate Tsg101 levels in vivo (Feng et al., 2000). Aberrant cellular phenotypes are observed if single components of ESCRT-I are overexpressed or depleted (Doyotte et al., 2005; Goila-Gaur et al., 2003; Johnson et al., 2005).

There are many parallels between yeast and human ESCRT-I regarding its core function. However, additional human Vps37 isoforms may provide extra functionalities for ESCRT-I. Discovery of new ESCRT-I-interacting partners, such as AIP/ALIX, which binds directly to ESCRT-III, provides extra branches in the human ESCRT network not apparent in yeast (Strack et al., 2003; von Schwedler et al., 2003). Other recently characterized ESCRT-I binding partners, such as TOM1L1, SIMPLE, and Tal, suggest additional layers of regulation not yet well understood (Amit et al., 2004; Puertollano, 2005; Shirk et al., 2005).

Viruses usurp endogenous ESCRT-I to promote their budding (reviewed in Demirov and Freed, 2004; Morita and Sundquist, 2004). Partial suppression of an ESCRT-I mutant class E phenotype can be achieved by overexpression of ESCRT-II, suggesting that ESCRT-I acts upstream of ESCRT-II (Babst et al., 2002b).

Yeast ESCRT-II is composed of three proteins, Vps22, Vps25, and Vps36, and the structure of the yeast ESCRT-II core showed a trilobal arrangement of these tightly associated subunits (Hierro et al., 2004; Teo et al., 2004a). Although the biological role of ESCRT-II has been most thoroughly studied in yeast, it was shown recently that ESCRT-II plays an important role in *Drosophila* since mutations in the Vps25 subunit of ESCRT-II activate Notch and Dpp receptor signaling due to endosomal accumulation of these receptors (Thompson et al., 2005; Vaccari and Bilder, 2005). The yeast Vps36 subunit of ESCRT-II binds ubiquitin using one of its two NZF zinc fingers in its N-terminal region, with an affinity comparable to the ubiquitin/UEV ESCRT-I interaction (Alam et al., 2004; Meyer et al., 2002). Surprisingly, the N-terminal region of the human Vps36, EAP45, also binds ubiquitin despite having no NZF domain (Slagsvold et al., 2005). ESCRT-II also directly interacts with ESCRT-III via a Vps25(EAP20)/Vps20(CHMP6) interaction (Teo et al., 2004a; Yorikawa et al., 2005).

ESCRT-III consists of four subunits, Vps2, Vps20, Vps24, and Snf7. ESCRT-III subunits associate with endosomal membranes in multiple ways: via the myristoyl group of Vps20 (Babst et al., 2002a); a Vps20-dependent interaction with ESCRT-II (Teo et al., 2004a); a direct interaction between Snf7 and membranes (Lin et al., 2005); and binding of Vps24 to PtdIns(3,5)P<sub>2</sub> (Whitley et al., 2003). ESCRT-III recruits accessory proteins such as Bro1/Alix (Bowers et al., 2004; Katoh et al., 2003; Kim et al., 2005; Martin-Serrano et al., 2003a; Peck et al., 2004; von Schwedler et al., 2003), which in turn recruits the deubiquitinase Doa4 (Luhtala and Odorizzi, 2004). Finally, the AAA-type ATPase Vps4 disassembles the whole machinery (Babst et al., 1998; Scott et al., 2005).

The importance of phosphoinositides in the MVB pathway was first shown with the discovery that Vps34, a class III PI-3-kinase producing PtdIns3P, is essential for protein sorting (Schu et al., 1993). Inhibition of Vps34 with wortmannin or antibodies causes defects in MVB formation (Fernandez-Borja et al., 1999; Futter et al., 2001). PtdIns3P is highly enriched in early endosomes and in the luminal vesicles of MVBs, where it recruits proteins through interactions with several specialized lipid binding domains (Gillooly et al., 2000).

Three main groups of players in the MVB protein sorting pathway have been identified: transmembrane ubiquitinated cargo, phospholipids, and machinery that reversibly associates with endosomes. To elucidate what drives the progression of ubiquitinated cargo along this pathway, we need not only a clear directory of the components involved but also the architecture of the individual components, and their interconnections. Here we describe the structure

of the conserved ESCRT-I core, which explains numerous observations previously reported. Furthermore, we provide evidence that ESCRT-I makes a stable, direct interaction with ESCRT-II in vitro. This is achieved through the N-terminal (non-ubiquitin binding) NZF finger, which is part of the double NZF-finger insertion within the GLUE domain of Vps36. From the crystal structure, we show that the GLUE domain is a split PH domain, and we demonstrate its ability to bind PtdIns3P and translocate to endosomes in vivo. Importantly, GLUE domain mutations that inhibit lipid binding also inhibit sorting of ubiquitinated cargo into the yeast vacuole.

## RESULTS

### ESCRT-I Core Expression and Crystallization

The three subunits of the *S. cerevisiae* ESCRT-I complex were coexpressed in *E. coli* using a polycistronic expression vector. Various domain boundaries for each subunit were tried, guided either by proteolytic products generated during expression of a full-length complex or sequence analysis of conserved domain boundaries. Expression trials converged on a stable heterotrimeric complex formed by the C-terminal regions of Vps23 (residues 305–385) and Vps37 (residues 130–213) and the N-terminal region of Vps28 (residues 1–147) (See Supplemental Data). Complexes were purified through an N-terminal His<sub>6</sub> tag on Vps28 and crystallized in space group P6<sub>1</sub> (a = 167.9, c = 50.2).

The structure was solved by MAD with a SeMet-substituted crystal. Although the resolution was low, 3.6 Å, this dataset enabled unambiguous assignment of all three subunits. To assign a reliable sequence register, we introduced 11 sequence landmarks by mutagenesis of endogenous hydrophobic residues into methionine and by soaking crystals with cysteine-reactive heavy metals. There are two heterotrimers in the asymmetric unit, with only small differences in the extent of ordered residues at the C termini of Vps28 subunits and the N termini of Vps37 subunits.

### ESCRT-I Core Structure

The low-resolution structure of the heterotrimeric ESCRT-I core enabled us to determine the fold and arrangement of individual subunits and identify a few critical interactions that maintain this tight heterotrimeric complex. The heterotrimeric ESCRT-I core consists of one copy each of Vps23, Vps28, and Vps37. The structure is primarily composed of three long, parallel helical hairpins, each corresponding to a different subunit (Figure 1A). Each hairpin forms a rib in a splayed fan, where Vps23 is the middle rib making direct interactions with the Vps28 subunit on one side and Vps37 subunit on another. The loops of the three hairpins converge at the stem of the fan while the N and C termini of all subunits radiate from the outer rim, except for the C terminus of Vps28, which has three additional small helices that fold back and pack against its own

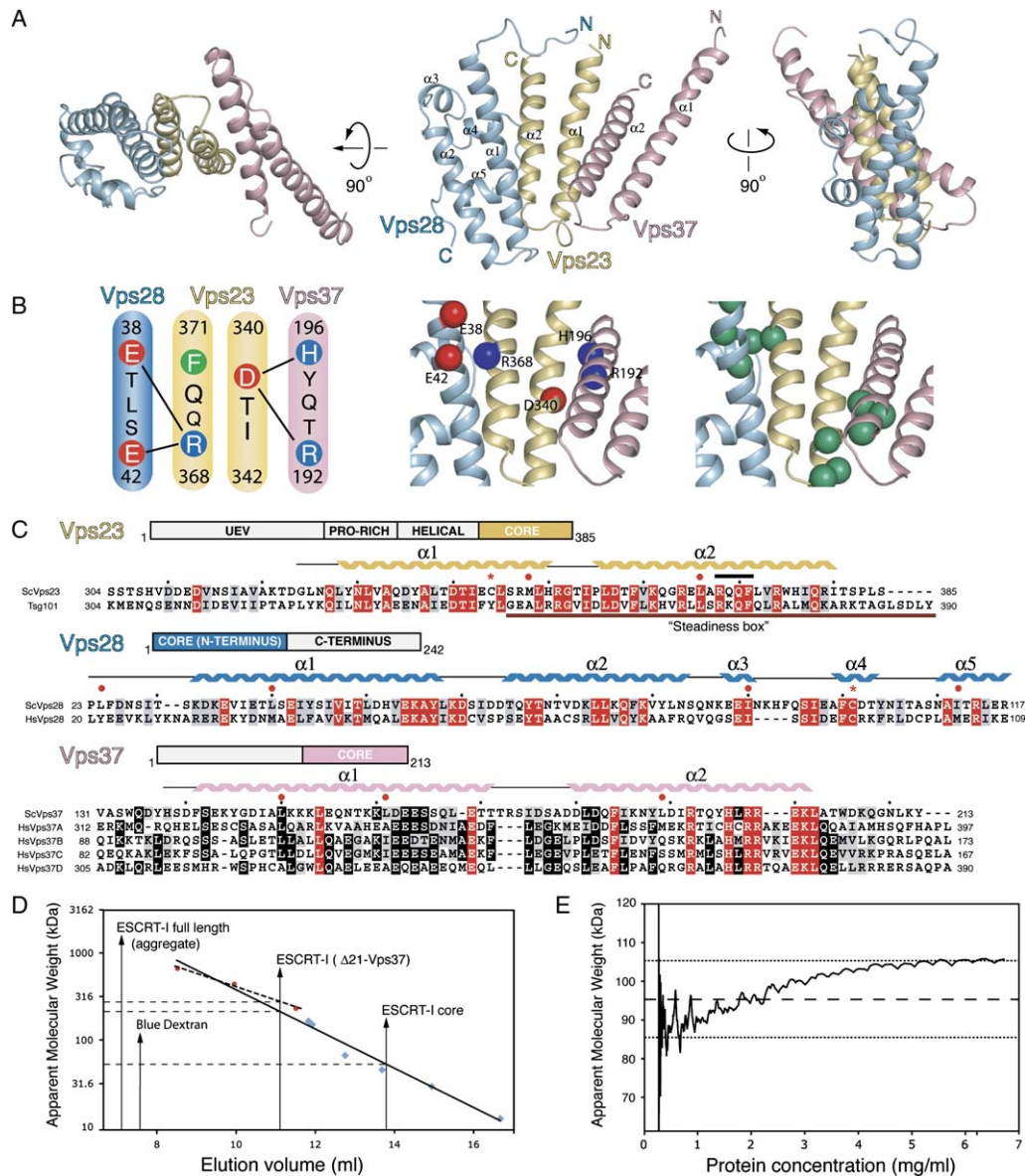


**Figure 1. The Crystal Structure of Yeast Heterotrimeric ESCRT-I Core Consists Principally of Three Helical Hairpins**

(A) Three orthogonal views of the fan-shaped ESCRT-I core (PyMol).

(B) The conserved sequence motifs involved in intersubunit interactions. Electrostatic interactions are shown schematically (left panel) and on the ESCRT-I core structure (middle panel), with basic residues shown as blue spheres and acidic residues as red. Additional hydrophobic clusters involved in tight association of these subunits are marked by green spheres (right panel): in the Vps23/Vps28 interface, Phe371<sup>Vps23</sup>/Ile37<sup>Vps28</sup>, Leu40<sup>Vps28</sup>, Tyr44<sup>Vps28</sup>, Tyr104<sup>Vps28</sup>, and in the Vps23/Vps37 interface, Leu345<sup>Vps23</sup>, Met348<sup>Vps23</sup>, Ile354<sup>Vps23</sup>/Leu181<sup>Vps37</sup>, Phe184<sup>Vps37</sup>, Ile185<sup>Vps37</sup>.

(C) Sequence alignment of ESCRT-I yeast (Sc) and human (Hs) subunits. Landmarks that assisted in sequence assignment are shown as red circles (SeMet) or asterisks (cysteines). The “steadiness box” (brown line) and the 368-RKQF-371 motif (black line) in Tsg101 are marked.

(D) Gel filtration of full-length ESCRT-I, ESCRT-I ( $\Delta 21$ -Vps37), and ESCRT-I core on a Superdex 200 HR10/30. Apparent size of ESCRT-I ( $\Delta 21$ -Vps37) was determined by comparison against either a complete set of gel filtration standards (12.4 to 669 kDa, solid line) or a subset of higher molecular weight markers (232 to 669 kDa, dashed line). The apparent size of ESCRT-I ( $\Delta 21$ -Vps37) is 214–280 kDa.

(E) Equilibrium analytical ultracentrifugation of ESCRT-I ( $\Delta 21$ -Vps37) shows an average apparent size of 105 kDa, well in agreement with an expected size of a 1:1:1 complex (94.7 kDa).

hairpin. No direct interactions between Vps28 and Vps37 are observed in the ESCRT-I core.

The most prominent intersubunit interactions between the subunits are hydrophobic. Vps23 makes extensive

contacts to both Vps28 (2900 Å<sup>2</sup>) and Vps37 (2700 Å<sup>2</sup>). The primary contact region between Vps23 and Vps28 involves helix  $\alpha 2$  in Vps23 and helix  $\alpha 1$  from Vps28. The major contact between Vps23 and Vps37 involves a stretch of

helix  $\alpha 1$  and a subsequent loop from Vps23 packing against helix  $\alpha 2$  from Vps37. Vps37 has a longer N-terminal helix that points away from the structural core. It corresponds to the most divergent region of the ESCRT-I core among different species, consistent with it making no direct interactions with other regions of Vps37 or the ESCRT-I subunits.

At the heart of the Vps23/Vps28 interface is the 368-RQQF-371 motif from Vps23, with Arg368<sup>Vps23</sup> sandwiched between two acidic residues, Glu38 and Glu42 from Vps28. These charged residues are completely conserved (Figures 1B and 1C). Furthermore, Phe371<sup>Vps23</sup> inserts into a hydrophobic dimple on Vps28 lined with Ile37, Leu40, Tyr44, and Tyr104. Mutation of the analogous tetrapeptide motif in human Tsg101 (368-RKQF-371) completely eliminated the interaction with Vps28 and the function of ESCRT-I in viral budding (Martin-Serrano et al., 2003b).

The Vps23/Vps37 interface is centered on salt links of invariant Asp340<sup>Vps23</sup> with conserved Arg192<sup>Vps37</sup> and His196<sup>Vps37</sup>. These basic residues are part of the most conserved sequence motif in Vps37, 192-R/KxxxHxRR-199, that maps to the intersection of the Vps23/Vps37 hairpins. An adjacent hydrophobic patch (between Leu345<sup>Vps23</sup>/Met348<sup>Vps23</sup>/Ile354<sup>Vps23</sup> and Leu181<sup>Vps37</sup>/Phe184<sup>Vps37</sup>/Ile185<sup>Vps37</sup>) further anchors this interface toward the stem of ESCRT-I. In addition to contacts within the ESCRT-I core, Vps37 has further interactions with the N-terminal region of Vps23/Tsg101, beyond the core structure (Bache et al., 2004; Eastman et al., 2005; Stuchell et al., 2004).

The steadiness box, residues 346–390 in Tsg101, was shown previously to be important for regulating steady-state levels of Tsg101 in vivo via a posttranslational mechanism (Feng et al., 2000). The steadiness box alone is required but not sufficient for this activity. This region maps to half of the Vps23 hairpin, including the  $\alpha 1$ - $\alpha 2$  loop and the entire  $\alpha 2$  helix. Perhaps the simplest explanation for the effect of the steadiness box on endogenous Tsg101 levels, is that overexpression of exogenous Tsg101 sequesters endogenous Tsg101 binding partners (Vps28 and Vps37), resulting in degradation of the free endogenous Tsg101.

### ESCRT-I Appears to Be a 1:1:1 Complex that Runs Anomally on Gel Filtration

Several previous studies have estimated the size of endogenous yeast ESCRT-I as approximately 350 kDa (Babst et al., 2000; Katzmann et al., 2001). In light of the ESCRT-I core structure having a 1:1:1 ratio of the three subunits, we reinvestigated the stoichiometry of the intact ESCRT-I. When intact ESCRT-I is expressed in *E. coli*, a significant proportion of the purified complex has 21 residues clipped from the N terminus of Vps37. Surprisingly, this has a dramatic effect on the apparent molecular weight of the complex by gel filtration. The intact ESCRT-I runs as an aggregate, which elutes earlier than the 670 kDa thyroglobulin protein standard. In contrast, the ESCRT-I with

this small N-terminal deletion elutes with an apparent molecular weight of 214–280 kDa (depending on the sets of standards chosen) (Figure 1D). Given that this N-terminal region is absent even in fungi other than *S. cerevisiae*, we concentrated further analysis on the clipped complex. To facilitate purification of this complex, Vps37 ( $\Delta 1$ –21) was engineered and coexpressed with intact Vps23 and Vps28, and this complex was used throughout this study (ESCRT-I ( $\Delta 21$ -Vps37)).

Unexpectedly, the ESCRT-I complex ( $\Delta 21$ -Vps37), with an apparent molecular weight of 214–280 kDa by gel filtration (Figure 1D), has a much smaller size by equilibrium analytical ultracentrifugation, with the average apparent molecular weight of approximately 105 kDa (Figure 1E). A direct fitting of the data revealed a major component of  $85 \pm 0.2$  kDa ( $1\sigma$ ) with a minor 170 kDa component. The expected size for the ESCRT-I ( $\Delta 21$ -Vps37) with a 1:1:1 stoichiometry is 94.7 kDa. Therefore, it appears that the ESCRT-I forms a 1:1:1 ternary complex. The long duration of ultracentrifugation did not affect complex integrity as judged by gel filtration and SDS gel electrophoresis. The presence of a minor heavier species could represent a small fraction of dimeric ESCRT-I.

### ESCRT-II Interacts Directly with ESCRT-I

Yeast two-hybrid studies have identified interactions between ESCRT-I and ESCRT-II (Bowers et al., 2004; von Schwedler et al., 2003). However, it is currently unclear whether ESCRT-I and ESCRT-II interact directly or through an adaptor protein. To test whether these two complexes can directly interact in vitro, we used analytical gel filtration and recombinant yeast ESCRT-I and ESCRT-II, expressed and purified from *E. coli*. ESCRT-I and ESCRT-II coelute with an apparent molecular weight higher than those of individual complexes (Figure 2A), indicating that ESCRT-I and ESCRT-II can form a direct and stable “super-complex” in vitro. We have also mapped the region of ESCRT-I/ESCRT-II interactions to the C terminus of Vps28 (ESCRT-I subunit, residues 148–242) and the N terminus of Vps36 (ESCRT-II subunit, residues 1–289). The N-terminal region of human Vps36 (EAP45) was recently named the GLUE domain (GRAM-like, ubiquitin binding in EAP45) (Slagsvold et al., 2005), and therefore we will refer to the corresponding 1–289 region of yeast Vps36 as a GLUE domain. The C terminus of Vps28 is sufficient for interaction with the Vps36 GLUE domain as shown by gel filtration (Figure 2B). Furthermore, when coexpressed in *E. coli*, the nontagged Vps36 GLUE domain can be copurified with a His<sub>6</sub>-tagged Vps28 C terminus (Figure 2C). Preliminary analysis of gel filtration results suggests a 1:1 stoichiometry. To further map the region of interaction in Vps36, we compared the intact GLUE domain (residues 1–289) with an engineered deletion variant from which a yeast-specific insertion encompassing residues 100–251 is removed. In contrast to the intact GLUE domain, this deletion variant did not form a complex with the C terminus of Vps28 (Figure 2D). We next tested whether the GLUE domain

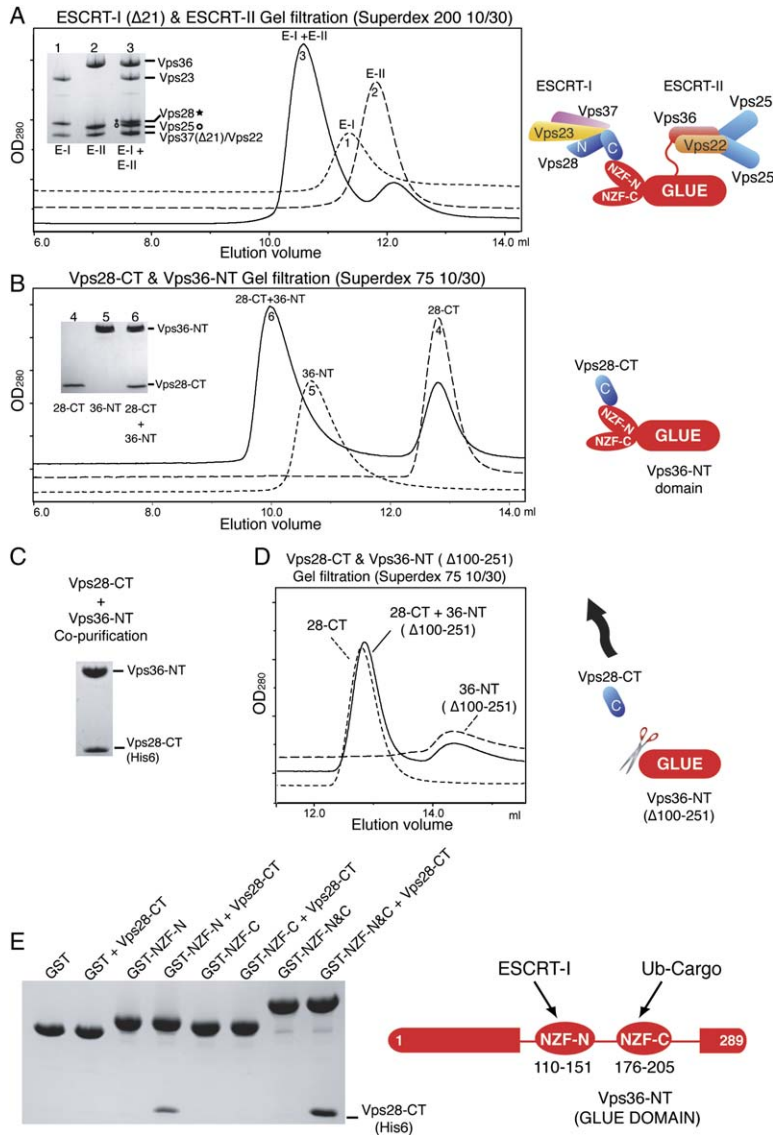


**Figure 2. The Vps28 C Terminus of Yeast ESCRT-I Interacts Directly with the N-Terminal NZF Zinc Finger within the Vps36 GLUE Domain of ESCRT-II**

(A) Gel filtration showing a direct interaction between ESCRT-I ( $\Delta 21$ -Vps37) and ESCRT-II. Elution profiles of ESCRT-I ( $\Delta 21$ -Vps37) alone (Peak 1), ESCRT-II alone (Peak 2), and a mixture of ESCRT-I ( $\Delta 21$ -Vps37) with ESCRT-II (Peak 3). Both ESCRT-I and ESCRT-II shift to a higher molecular weight peak when mixed together, indicating formation of a super-complex. SDS-PAGE of samples from each gel filtration peak are shown in the inset.

(B) Elution profiles of the C-terminal region of Vps28 alone (Vps28-CT, residues 148–242) (Peak 4), the GLUE domain of Vps36 alone (Vps36-NT, residues 1–289) (Peak 5), and a mixture of Vps28-CT with Vps36-NT (Peak 6). Peak fractions were analyzed by SDS-PAGE and stained with Coomassie.

(C) When coexpressed in *E. coli*, His<sub>6</sub>-tagged Vps28-CT and nontagged Vps36-NT can be copurified by affinity chromatography and gel filtration.

(D) Elution profile of Vps28-CT and Vps36-NT (with an internal deletion of residues 100–251) mixed together did not show a shift to a higher molecular weight peak, indicating that the insertion is necessary for interaction.

(E) GST-tagged GLUE domain insertion containing both zinc fingers (residues 110–205) is sufficient to bind Vps28-CT. The isolated Vps36-NZF-N finger (residues 110–151) binds directly to Vps28-CT, whereas the isolated Vps36-NZF-C finger (residues 176–205) does not.

insertion is sufficient for the interaction with the Vps28 C terminus. GST-tagged GLUE domain insertion (residues 110–205) pulls down the His-tagged Vps28 C terminus (Figure 2E). As the GLUE domain insertion contains two zinc fingers (NZF-N: residues 110–151 and NZF-C: residues 176–205), we tested each NZF individually for binding to Vps28. Isolated GST-NZF-N binds to the His-tagged Vps28 C terminus, while the isolated GST-NZF-C does not (Figure 2E). Therefore, the two NZF fingers from Vps36 have different functions: NZF-N binds to ESCRT-I and NZF-C binds to ubiquitin.

**ESCRT-II Preferentially Binds to PtdIns3P-Containing Lipid Vesicles**

Given that ESCRT-II localizes to endosomes in vivo (Slagsvold et al., 2005), we wanted to investigate whether it can interact with membranes directly. We previously

showed that the ESCRT-II core complex (lacking Vps36 residues 1–370) binds efficiently to Folch lipids in vitro only in the presence of the ESCRT-III-Vps20 subunit (Teo et al., 2004a). We have now examined the binding of full-length ESCRT-II to lipid vesicles.

In contrast to the ESCRT-II core, the full-length ESCRT-II binds efficiently to lipid vesicles made of Folch lipids (Figure 3A). No binding to synthetic liposomes made of PC/PE/PS/cholesterol is observed. Folch lipids constitute a mixture of phosphoinositides and other lipids isolated from bovine brains. To define the lipid specificity of ESCRT-II/membrane interaction, we carried out binding assays with vesicles having a defined lipid composition (Figure 3B). Full-length ESCRT-II binds most efficiently to PtdIns3P-containing lipid vesicles but also significantly to PtdIns(3,4)P<sub>2</sub> and moderately to PtdIns(4)P and PtdIns(3,5)P<sub>2</sub>. These results suggest that ESCRT-II has

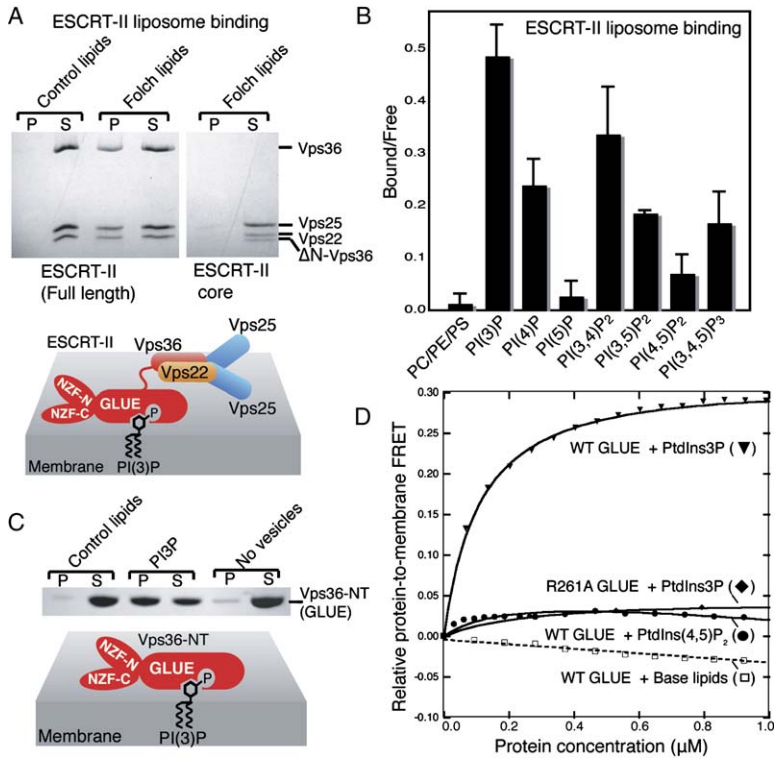


**Figure 3. ESCRT-II Binds PtdIns3P via Its GLUE Domain**

(A) Comparison of full-length ESCRT-II and ESCRT-II core (residues 1–370 deleted,  $\Delta$ N-Vps36) binding to Folch lipids or to control liposomes (PC/PE/PS/cholesterol). P and S indicate “pellet” and “supernatant” fractions after ultracentrifugation, analyzed by SDS-PAGE and Coomassie staining.

(B) Phosphoinositide specificity of full-length ESCRT-II using vesicles containing 10% of various phosphoinositides. The ratios represent averages of three independent assays. Error bars represent standard deviations of the averages.

(C) Isolated Vps36 GLUE domain (residues 1–289) is sufficient for binding to PtdIns3P-containing liposomes.

(D) Lipid binding by the isolated Vps36 GLUE domain (residues 1–289) measured from intrinsic tryptophans to the DANSYL probe of the DANSYL-PS-containing liposomes (PC/PE/DANSYL-PS/cholesterol/phosphoinositide). The “base” lipids contain an additional 10% PC instead of a phosphoinositide.

the ability to associate with membranes independently of ESCRT-I and ESCRT-III.

### The GLUE Domain of Vps36 Is Sufficient for Liposome Binding

Because the ESCRT-II core (lacking N-terminal 1–370 residues of Vps36) shows little tendency to interact with membranes on its own, we suspected that the PtdIns3P interaction of the full-length ESCRT-II was due to the N terminus of Vps36. Indeed, the yeast Vps36 GLUE domain binds to PtdIns3P-containing vesicles similarly to the full-length ESCRT-II complex (Figure 3C). The apparent affinity of the GLUE domain for PtdIns3P-containing vesicles is approximately 0.1  $\mu$ M (Figure 3D). Since endosomal membranes are highly enriched in PtdIns3P, our results suggest that the Vps36 GLUE domain may participate in endosomal localization. The human Vps36 was shown recently to bind to PtdIns(3,4,5)P<sub>3</sub> through its N-terminal GLUE domain (Slagsvold et al., 2005).

The structural prediction using the Robetta server (Zhou and Zhou, 2005) suggested that the yeast Vps36 GLUE domain has a fold that is similar to the PH domain of dynamin, with a large insertion encompassing residues 100–250 between the putative PH domain strands six and seven (Figure 4A). This insertion contains two NZF zinc fingers and is present in all fungi, but not in metazoa. Stenmark and colleagues also predicted a PH domain-like character of the N terminus of the human Vps36 (Slagsvold et al., 2005). As the Vps36 PH domain was not recognized in a recently reported genome-wide analysis of

yeast PH domains (Yu et al., 2004), almost certainly due to the large, 150 residue NZF-containing insertion (an insertion as large as the PH domain itself), we wanted to gain a direct proof that it has a split PH domain fold by X-ray crystallography. Attempts to crystallise the intact GLUE domain of Vps36 were not successful. Therefore, we engineered a construct missing the yeast-specific insertion (encompassing residues 1–99 directly fused to residues 252–289). The engineered protein crystallized in space group P2<sub>1</sub>2<sub>1</sub>2 (a = 94.5, b = 88.4, and c = 45.9), with two molecules in the asymmetric unit.

### The GLUE Domain of Yeast Vps36 Has a PH-Domain Fold

The 1.9 Å structure was solved by MAD with a SeMet-substituted crystal. The structure has a typical PH domain architecture with two curved  $\beta$  sheets and one long  $\alpha$  helix (Figure 4C). The two sheets ( $\beta$ 1– $\beta$ 4 and  $\beta$ 5– $\beta$ 7) form a  $\beta$  barrel-like structure. The C-terminal  $\alpha$  helix is wedged between the two  $\beta$  sheets, covering a hydrophobic core. Although split PH domains have been proposed previously (reviewed in Lemmon, 2005), our structure provides the evidence that the GLUE domain indeed has a split PH-domain fold. The site of the insertion is located away from the putative membrane binding surface and is not occluding the lipid binding pocket.

The crystal structure reveals a distinct, highly positively charged pocket occupied by a single sulfate anion (Figure 4C). The walls of the pocket are built by three loops,  $\beta$ 1/ $\beta$ 2,  $\beta$ 5/ $\beta$ 6, and  $\beta$ 7/ $\alpha$ 1. The sulfate ion is pinned from

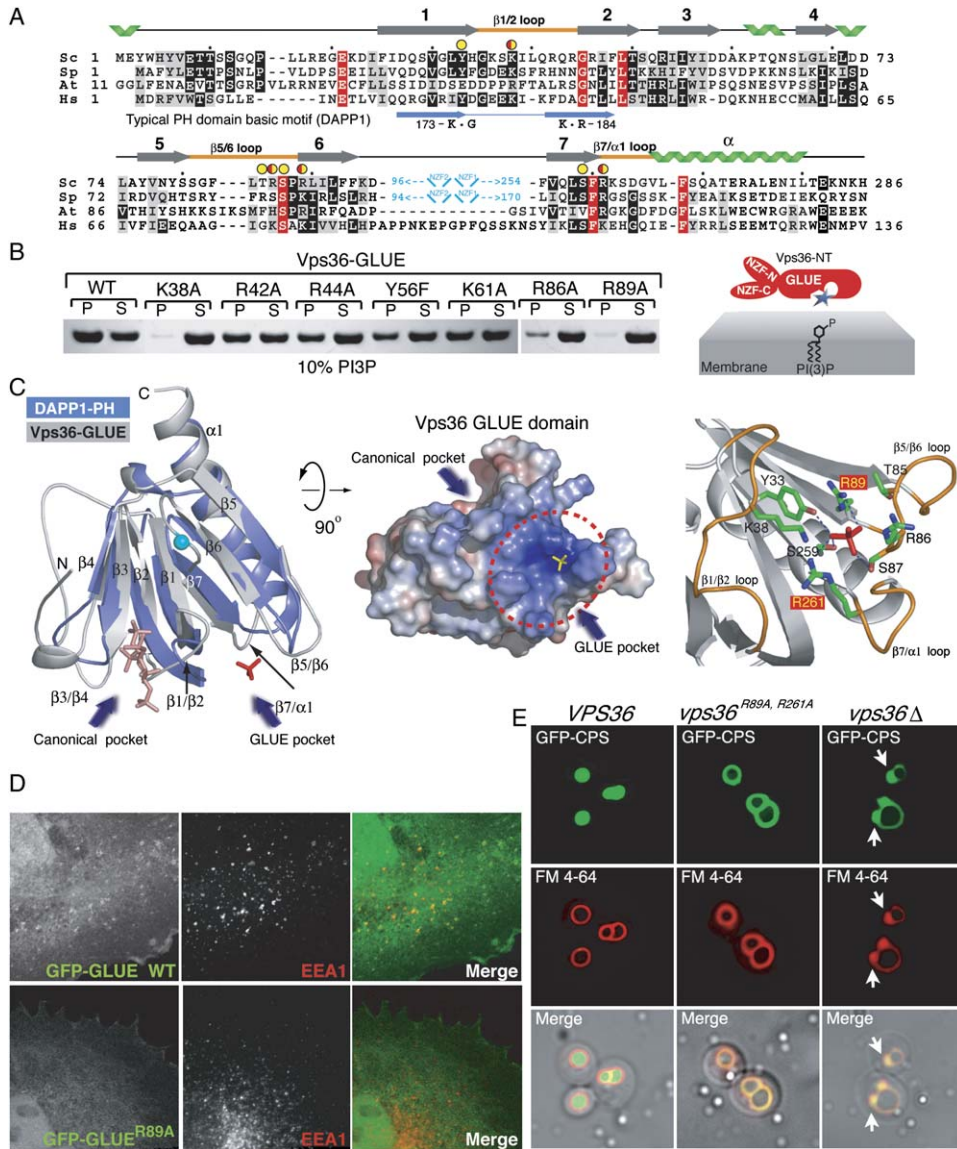


**Figure 4. Vps36 GLUE Domain Is a Split PH Domain with a Noncanonical Lipid Binding Pocket**

(A) Sequence alignment of Vps36 GLUE domains from *S. cerevisiae* (Sc), *S. pombe* (Sp), *A. thaliana* (At), and *H. sapiens* (Hs). Red spheres indicate residues that decrease binding to PtdIns3P vesicles when mutated. Yellow spheres indicate residues within 4 Å of the sulfate anion in the lipid binding pocket. The sequence motif for high-affinity phosphoinositide binding to canonical PH domains is illustrated with the example of DAPP1 below the alignment.

(B) The GLUE domain mutants were tested for binding to 10% PtdIns3P lipid vesicles by sedimentation assay.

(C) The PH domain of DAPP1 (1FAO) (slate) in complex with Ins(1,3,4,5)P<sub>4</sub> (Ferguson et al., 2000) is superimposed on the Vps36 GLUE domain (white). Ins(1,3,4,5)P<sub>4</sub> in the DAPP1 structure occupies a canonical phosphoinositide binding pocket. The sulfate anion in Vps36 GLUE domain resides in a distinct noncanonical pocket. A cyan sphere marks the position of a large insertion (residues 100–251), which was removed from this construct (left panel). Surface electrostatic potential of the GLUE domain shows a basic lipid binding pocket marked by the sulfate anion (yellow sticks) (middle panel). Closeup view of the interactions with the sulfate in the phosphoinositide binding pocket in the Vps36 GLUE domain (right panel) is shown. Residues within 4 Å of the sulfate ion are shown as sticks.

(D) Subcellular distribution of yeast Vps36 GFP-GLUE domain, either wild-type (wt) or R89A mutant, transiently overexpressed in COS-7 cells. Only wild-type GFP-GLUE domain shows punctate distribution. The endogenous EEA1 (red), an early endosomal marker, partially colocalizes with the wild-type GFP-GLUE domain, as shown in the merged image (yellow puncta).

(E) The full-length Vps36 with an R89A, R261A double mutation in the lipid binding pocket exhibits a strong defect in GFP-CPS cargo sorting into vacuoles in the context of *vps36Δ* strain. The GFP-CPS hybrid protein is missorted to the limiting membrane (labeled by FM4-64) of the vacuole. Unlike the *vps36Δ* strain, the double mutant does not accumulate prevacuolar endosomes (arrow heads), indicating that MVB sorting is not completely defective in the double mutant.

two sides by the conserved Arg89 (from  $\beta 5/\beta 6$  loop) and Arg261 (from  $\beta 7/\alpha 1$ ) (Figure 4C). The charge distribution and the position of the sulfate ion are consistent with this pocket being a lipid headgroup binding pocket responsible for the observed ability of the Vps36 GLUE domain to bind PtdIns3P. Modeling of PtdIns3P into this pocket suggests that Arg89 and Arg261 are putative ligands of the 3-phosphate and that Lys38 and Arg86 also form a part of this pocket. Indeed, the R89A and R261A mutants failed to bind PtdIns3P, while the K38A and R86A mutants showed reduced lipid binding (Figures 3D and 4B). In contrast, mutations of residues in the region analogous to the “canonical” PH phosphoinositide binding pocket, Arg42, Arg44, Tyr56, and Lys61, did not significantly affect lipid binding (Figure 4B). This Vps36 GLUE phosphoinositide pocket is clearly different than the pocket between the  $\beta 1/\beta 2$ ,  $\beta 3/\beta 4$ , and  $\beta 6/\beta 7$  loops used by the vast majority of characterized PH domains (Figure 4C) (Ferguson et al., 2000; Lietzke et al., 2000). The only known exceptions to the canonical phosphoinositide binding pocket are the PH domains of  $\beta$ -spectrin (Hyvonen et al., 1995) and the Tfb1/p62 subunit of TFIIH (Di Lello et al., 2005), which bind phosphoinositides in a pocket on the opposite side of the  $\beta 1/\beta 2$  “fence,” involving the  $\beta 5/\beta 6$  and  $\beta 7/\alpha 1$  loops. Previous analysis of lipid binding by PH domains (Ferguson et al., 2000) showed that phosphoinositides are recognized by a characteristic sequence motif consisting of a Lys in strand  $\beta 1$  followed by a K/R-x-R motif in strand  $\beta 2$ . Superimposing the structure of the Vps36 GLUE domain on a PH domain with a “canonical” phosphoinositide binding site, e.g., DAPP1, shows that the Vps36 GLUE domain does not have basic residues equivalent to this motif (Figure 4A).

#### GLUE Domain of Yeast Vps36 Is Sufficient for Recruitment to Endosomes

To test the physiological relevance of the observed ability of the isolated Vps36 GLUE domain to bind to PtdIns3P in vitro, we examined the cellular distribution of the GFP-tagged yeast Vps36 GLUE domain (1–289) transfected into COS-7 cells. While the wild-type GLUE domain has a punctate distribution throughout the cytosol, the point mutant in the lipid binding pocket, R89A, which does not bind to lipids in vitro, shows a diffuse cytosolic staining. The wild-type GLUE domain partially colocalized with early endosomal marker EEA1, suggesting that these puncta are endosomal structures (Figure 4D). Furthermore, we tested a double mutant in the lipid binding pocket, Vps36<sup>R89A,R261A</sup>, for its effects on vacuolar sorting in yeast. This mutant, when expressed in a yeast strain lacking Vps36 (*vps36 $\Delta$* ) results in strong missorting of GFP-CPS cargo to the limiting membrane of the vacuole (Figure 4E). This demonstrates that the lipid binding activity of the Vps36 GLUE domain plays an important role in MVB cargo sorting. However, unlike cells lacking Vps36, the *vps36*<sup>R89A,R261A</sup> mutant does not result in the accumulation of endosomal membranes (class E dot), suggesting that MVB sorting is not completely disrupted. The stronger

phenotype of the *vps36 $\Delta$*  mutant is probably due to loss of protein-protein interactions, such as with ESCRT-I and ESCRT-III, in addition to loss of membrane interactions.

#### ESCRT-II Binding to ESCRT-I, Ubiquitin, and Lipid Is Not Competitive

Since the GLUE domain of Vps36 combines three different binding activities, to phosphoinositides, ESCRT-I, and ubiquitin, we asked whether these interactions can occur at the same time or are mutually exclusive. We first examined whether ESCRT-II can simultaneously interact with ESCRT-I and liposomes. Purified ESCRT-I alone does not bind lipid vesicles (Figure 5A). However, ESCRT-I preincubated with the full-length ESCRT-II before addition to lipid vesicles, cosedimented with ESCRT-II/liposomes (Figure 5A). Similarly, preincubation with the Vps36 GLUE domain (Vps36-NT) causes ESCRT-I to cosediment with lipid vesicles (Figure 5A). ESCRT-I does not cosediment with either the full-length ESCRT-II or the Vps36 GLUE domain when the C terminus of Vps28 (ESCRT-I) is deleted (Figure 5B). These results show that the interaction between the Vps28 C terminus and the Vps36 GLUE domain is both necessary and sufficient to recruit ESCRT-I to lipid vesicles.

In yeast, recognition of ubiquitin by ESCRT-II is mediated by the GLUE domain of Vps36, which contains two NZF domains, one of which (NZF-C, residues 177–205) binds ubiquitin (Alam et al., 2004). GST-ubiquitin does not affect lipid binding of ESCRT-II, and it efficiently cosediments with ESCRT-II bound to lipid vesicles (Figure 5C). Similar results were observed with the isolated Vps36 GLUE domain (Figure 5D). An I44A mutation of ubiquitin that abolishes ubiquitin interaction with many ubiquitin binding modules (reviewed in Hicke and Dunn, 2003) eliminates cosedimentation with ESCRT-II (Figure 5C). Similarly, a mutation in the Vps36 NZF domain (T187G/F188S) that eliminates ubiquitin binding prevents ubiquitin from cosedimenting with the Vps36 GLUE/liposomes (Figure 5D). Finally, we tested whether ESCRT-II can interact with all three binding partners simultaneously. For these assays, we used an ESCRT-I complex with a deletion of the ubiquitin binding domain of Vps23 (ESCRT-I- $\Delta$ UEV) to prevent direct binding of ubiquitin to ESCRT-I. When incubated together, all of the partners cosedimented with vesicles (Figure 5E), suggesting that ESCRT-II is capable of interacting simultaneously with ESCRT-I (via NZF-N), ubiquitin (via NZF-C), and lipid vesicles (via PH domain) in vitro.

#### DISCUSSION

As a step toward understanding the progression of ubiquitinated membrane cargo from early endosomes to lysosomes, we provide insights into the architecture, membrane recruitment, and functional interactions of the ESCRT machinery driving this process. The conserved heterotrimeric ESCRT-I core is built from three copies of a common building block, a long helical hairpin, each

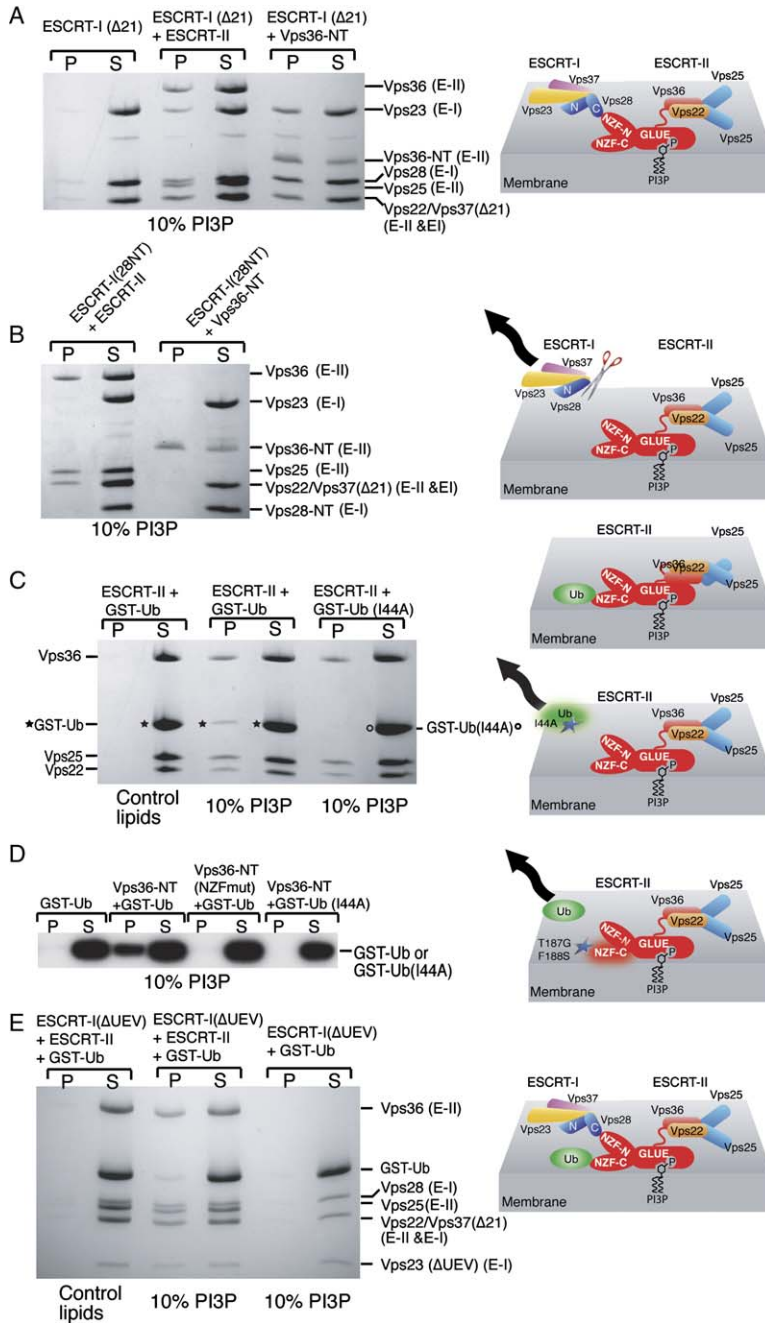


**Figure 5. ESCRT-II Can Simultaneously Interact with ESCRT-I, Ubiquitin, and Lipid Vesicles via Its Vps36 GLUE Domain**

(A) ESCRT-I alone or ESCRT-I mixed with ESCRT-II was incubated with PtdIns3P vesicles and sedimented by ultracentrifugation. ESCRT-I, on its own, does not sediment with PtdIns3P vesicles, but it does so in the presence of ESCRT-II or Vps36 GLUE domain (Vps36-NT).

(B) ESCRT-I with a deletion of the C-terminal region of the Vps28 subunit (148–242 deleted, ESCRT-I(Δ28NT)) does not interact with either ESCRT-II or the isolated GLUE domain.

(C) ESCRT-II can bind simultaneously to both ubiquitin (GST-Ub) and PtdIns3P but does not bind to control vesicles or to the mutant GST-Ub-I44A.

(D) The Vps36 GLUE domain is sufficient to cause GST-Ub to sediment with vesicles, and this is mediated by the NZF-C insertion in Vps36 because a mutation in NZF-C (T187G/F188S), shown to be defective in Ub binding (Alam et al., 2004), prevents GST-Ub from cosedimenting. GST-ubiquitin did not sediment on its own with PtdIns3P-containing vesicles. The GST-Ub was detected using a Western blot and an anti-GST antibody.

(E) ESCRT-II can bind simultaneously to ESCRT-I, ubiquitin, and lipid membranes. Full-length ESCRT-II was preincubated with GST-Ub and ESCRT-I (ΔUEV-EI, residues 1–251 deleted from Vps23) before addition to vesicles. Direct interactions of ESCRT-I (ΔUEV-EI) and ubiquitin with ESCRT-II is sufficient for their cosedimentation with vesicles. ESCRT-I (ΔUEV-EI) and ubiquitin alone do not interact and do not cosediment with vesicles.

corresponding to one of the three subunits. This core is necessary and sufficient for the assembly of the heterotrimeric 1:1:1 complex. The additional domains and motifs extending beyond the core serve as gripping tools for ESCRT-I critical functions. The ubiquitinated cargo is captured by the Vps23/Tsg101 UEV domain. The link to the upstream machinery, Vps27/Hrs, is also provided by the UEV domain (Pomillos et al., 2003) and, potentially, through interactions with Vps37 (Eastman et al., 2005). We show that a link to the downstream machinery is established by a direct interaction of a C-terminal domain

in Vps28 (ESCRT-I) and the NZF-N domain in the Vps36 subunit (ESCRT-II).

The interaction of ESCRT-I with Vps27/Hrs is required for efficient recruitment of ESCRT-I to early endosomes (Bache et al., 2003a; Katzmman et al., 2003). Vps27/Hrs also could have either a direct or an indirect role in activating ESCRT-I for its subsequent interaction with ESCRT-II. Our data now indicate that there could be an additional mechanism for ESCRT-I membrane recruitment, through an interaction with the GLUE domain from ESCRT-II, which itself binds to PtdIns3P. We propose that direct

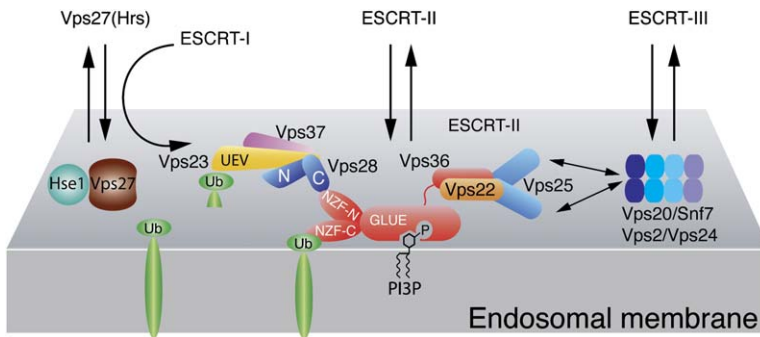


**Figure 6. A Scheme for the Dynamic Interplay between Membranes, Ubiquitinated Cargo, and the ESCRT Machinery Involved in Membrane Protein Sorting to Lysosomes**

Specific binding of Vps27/Hrs to PtdIns3P via its FYVE domain acts as an initial port of entry for ESCRT-I to early endosomes and potentially “primes” ESCRT-I for its subsequent interaction with ESCRT-II. Through its GLUE domain, ESCRT-II pulls ESCRT-I to late endosomes. ESCRT-I seems to be in a tug of war between Vps27/Hrs and the GLUE domain of ESCRT-II. Similarly, ESCRT-II is pulled by ESCRT-I on one side and by interactions with the Vps20 subunit from ESCRT-III on another. The upstream/downstream contest could be favored by a branching network to ESCRT-III since each of the two copies of Vps25 subunit from ESCRT-II can be pulled by an ESCRT-III.

interaction of ESCRT-I with ESCRT-II (itself linked to downstream ESCRT-III components) could be responsible for prolonged association of ESCRT-I with maturing endosomes. Interestingly, human ESCRT-I is found not only on early endosomes where it colocalizes with Hrs, but also on late endosomes from which Hrs is largely absent (Bache et al., 2003a). However, it is not clear whether this progression to late endosomes is mediated by direct interaction with Vps36 (which is found on late endosomes in mammalian cells Slagsvold et al., 2005) or by some other mechanism. Although the mammalian GLUE domain lacks this NZF insertion, it may have evolved an NZF-independent, alternative mechanism to bind ESCRT-I. The observation that the human Vps36 GLUE domain interacts with ubiquitin (Slagsvold et al., 2005), despite lacking the specialized yeast-specific Ub binding NZF finger, illustrates that similar surprises may await.

ESCRT-II (through its GLUE domain) binds not only to PtdIns3P but also significantly to PtdIns4P, PtdIns(3,4)P<sub>2</sub>, and PtdIns(3,5)P<sub>2</sub>. The broader specificity of the GLUE domain for phosphoinositides, when compared to Vps27/Hrs, which selectively binds to PtdIns3P, could explain why there is only a partial overlap in endosomal localization of these components. In addition, each of the two Vps25 subunits present in ESCRT-II binds to Vps20, an ESCRT-III component, and this branching network of interactions could further contribute to broader ESCRT-II localization (Teo et al., 2004a). In summary, it is tempting to suggest that Vps27/Hrs and ESCRT-II represent stations for traffic of ESCRT-I from early to late endosomes. What remains puzzling is that ESCRT-I and ESCRT-II readily copurify *in vitro* yet do not appear to constitutively associate in cells (Babst et al., 2002a). It would be exciting if the association of these complexes is regulated *in vivo* by other factors, such as modification by phosphorylation/ubiquitination or by interactions with other proteins of the endosomal machinery.

Ironically, the Vps36 GLUE domain, which was not present in the previously determined ESCRT-II core structures

(Hierro et al., 2004; Teo et al., 2004a), turns out to be one of the busiest domains in ESCRT-II. We solved the crystal structure of the isolated Vps36 GLUE domain, providing the evidence that the GLUE domain has a split PH-domain fold. The GLUE domain acts as a central cog driving the endosomal ESCRT machinery, through simultaneous interactions with PtdIns3P-containing membranes, ubiquitin, and ESCRT-I. The Vps36 GLUE domain binds PtdIns3P via a positively charged lipid binding pocket, delineated by the variable loops  $\beta 1/\beta 2$ ,  $\beta 5/\beta 6$  and  $\beta 7/\alpha 1$ , in contrast to the vast majority of characterized PH domains, which use a different lipid binding pocket. The critical role of membrane binding by the GLUE domain is apparent from the strong defect in vacuolar sorting of CPS caused by mutations in the Vps36 lipid binding pocket. The emerging picture is that two main functions of the ESCRT machinery, binding of ubiquitinated transmembrane cargo and membrane recruitment, can be accomplished by more than one component of the sorting machinery (Figure 6). This could enable selective retention, enrichment, and clustering of ubiquitinated cargo and machinery during transition from early to late endosomes, despite the progressive loss of upstream components, such as Vps27/Hrs, which play a critical role in the initial ubiquitin sorting and ESCRT recruiting steps. Similar dynamic fluctuations in other endosomal components, such as Rabs, occur during early to late endosome progression (Rink et al., 2005). The multiple, reversible interactions between ubiquitinated cargo, membranes, and machinery, together with branching networks, such as between ESCRT-II and ESCRT-III, ensure an efficient continuum in protein and lipid sorting and, ultimately, MVB formation.

## EXPERIMENTAL PROCEDURES

### Plasmids

The sequences encoding *S. cerevisiae* Vps23, Vps28, and Vps37 (ESCRT-I) were PCR amplified from genomic DNA (ATCC 9763D) and cloned into the polycistronic, coexpression vector pOPC,

following the general cloning strategy described by Tan (Tan, 2001). The resulting construct has a MetAlaHis<sub>6</sub> affinity tag preceding residue Met-1 of Vps28. Vps28 was cloned into the first cassette, Vps23 into the second, and Vps37 in the third. Mutants were generated using a QuikChange Mutagenesis Kit (Stratagene). ESCRT-II subunits, Vps22, Vps25, and Vps36 were cloned as previously described (Teo et al., 2004a). The N-terminal fragment of Vps36 (residues 1–289) and a C-terminal fragment of Vps28 (residues 148–242) were cloned into pOPHT and expressed with an N-terminal MetAlaHis<sub>6</sub> tag. Ubiquitin was cloned into the pOPTG vector and expressed with an N-terminal GST tag. All constructs were verified by sequencing.

#### Protein Expression and Purification

ESCRT-I proteins were coexpressed in C41(DE3) cells, grown at 37°C to an OD<sub>600nm</sub> = 1.0, then induced with 0.3 mM IPTG at 16°C for 12 hr. ESCRT-II proteins were grown the same way but were induced at 37°C for 3 hr. Both ESCRT-I and ESCRT-II complexes were purified by Ni<sup>2+</sup>-affinity, Q-Sepharose, and gel filtration chromatography. The purified proteins eluted from gel filtration in 20 mM Tris (pH 7.4), 100 mM NaCl, and 2 mM DTT. For the isolated Vps36 GLUE domain, the buffer contained an additional 10 mM (NH<sub>4</sub>)<sub>2</sub>SO<sub>4</sub>.

The GST-fusion proteins for lipid binding assays were purified on Glutathione Sepharose (Amersham). The resin was washed with buffer A (50 mM Tris [pH 7.5, 4°C], and 2 mM DTT) followed by buffer B (50 mM Tris [pH 7.5], 200 mM NaCl and 5 mM β-mercaptoethanol). GST-fusions were eluted with buffer C (50 mM Tris [pH 8.5], 10 mM glutathione and 2 mM β-mercaptoethanol), concentrated and desalted using PD-10 columns (Amersham). Constructs containing NZF zinc fingers were purified in the presence of 10 μM ZnCl<sub>2</sub>.

#### ESCRT-I Analytical Gel Filtration and Equilibrium Analytical Ultracentrifugation

See Supplemental Data.

#### Crystallization of ESCRT-I Core and Vps36 GLUE Domain

Optimal crystals for the engineered ESCRT-I core were obtained at 17°C by mixing 20 mg/ml protein with a reservoir solution containing 8%–10% PEG 8000, 8%–9% ethylene glycol, 0.1 M HEPES (pH 7.0–8.0). Optimal crystals of the yeast Vps36 GLUE domain without the insertion (residues 1–99 directly fused to residues 252–289) were obtained at 17°C by mixing 6.5 mg/ml protein with a reservoir solution containing 6% glycerol, 0.1M CHES (pH 9.5), 1M (NH<sub>4</sub>)<sub>2</sub>SO<sub>4</sub>, and 0.2M NaCl. ESCRT-I core and ESCRT-II GLUE domain crystals were cryoprotected by increasing the concentration of ethylene glycol or glycerol, respectively, to 25%. Attempts to crystallize the complex of GLUE domain with soluble head group analogs (diC<sub>4</sub>-PtdIns3P), either by cocrystallization or by soaking into preformed crystals, were not successful, probably due to the presence of high (NH<sub>4</sub>)<sub>2</sub>SO<sub>4</sub>.

#### Data Collection, Phasing, and Model Refinement

MAD data sets were collected at ESRF beamline ID14-4 using an ADSC CCD detector. Data collection, phasing, and model refinement were carried as described in Supplemental Data.

#### Liposome Binding Assays

For sedimentation assays, synthetic lipid vesicles contained 50% PC (Avanti, 840053), 20% PE (Avanti, 830022), 10% PS (Avanti, 830032), 10% cholesterol (Sigma, 8667) and 10% of the test phosphoinositide (Avanti or Echelon). Control vesicles contained an additional 10% PC instead of the test lipid. Folch lipids were obtained from Sigma (Sigma, B1502). Phospholipids were dissolved in 1:1 chloroform:methanol containing 0.1% HCl for 15 min, dried with argon, and desiccated under vacuum for 1 hr. Lipids were rehydrated in a buffer containing 20 mM Tris pH 7.4, 100 mM NaCl, and 1 mM β-mercaptoethanol to a final concentration of 1 mg/ml followed by sonication. Sedimentation assays contained purified proteins (3–15 μM), 0.5 mM MgCl<sub>2</sub>, and 50 μl of 1 mg/ml lipid vesicles in 100 μl reactions. After 15 min at 4°C, reac-

tions were sedimented at 140,000 × g in a Beckman TLA100 rotor for 15 min at 4°C. The supernatants (S) and the pellets (P), resuspended in an equal volume of buffer, were analyzed by SDS-PAGE and stained with Coomassie. Lipid binding affinities were determined using FRET as described in Supplemental Data.

#### Pulldown Assays

Glutathione resin in a binding buffer (PBS with 0.05% Triton X-100, 1 μM ZnCl<sub>2</sub>, and 5 mM β-mercaptoethanol) was mixed with 250 μg of GST-tagged protein and 150 μg of His-tagged Vps28-CT and *E. coli* cytosol (8 mg/ml). The assay mix was incubated for 1 hr at 4°C and washed eight times with PBS/0.05% Triton X-100. Bound proteins were eluted with SDS sample buffer and analyzed by SDS-PAGE.

#### Supplemental Data

Supplemental data include one table and supplemental text and can be found with the article online at <http://www.cell.com/cgi/content/full/125/1/99/DC1/>.

#### ACKNOWLEDGMENTS

We thank Martin Walsh, Andrew McCarthy, Joanne McCarthy, Elena Micossi, Raimond Ravelli, Didier Nurizzo, and Gordon Leonard at BM14, ID14-4, ID23, and ID29 at ESRF; Samar Hasnain, Michele Cianci, and James Nicholson at Daresbury SRS for assistance at the beamlines 10 and 14.1; Mike Wilson and Wai-Ching Hon for help and useful discussions. H.L.T. is supported by the ASTAR-Singapore. D.J.G. is supported by a studentship from the MRC. J.S. is supported as a HHMI Research Associate. S.D.E. is supported as an investigator of the HHMI. This work was supported by the MRC (R.L.W.).

Received: October 6, 2005

Revised: December 1, 2005

Accepted: January 12, 2006

Published: April 6, 2006

#### REFERENCES

- Alam, S.L., Sun, J., Payne, M., Welch, B.D., Blake, B.K., Davis, D.R., Meyer, H.H., Emr, S.D., and Sundquist, W.I. (2004). Ubiquitin interactions of NZF zinc fingers. *EMBO J.* 23, 1411–1421.
- Amit, I., Yakir, L., Katz, M., Zwang, Y., Marmor, M.D., Citri, A., Shtiegmán, K., Alroy, I., Tuvia, S., Reiss, Y., et al. (2004). Tal, a Tsg101-specific E3 ubiquitin ligase, regulates receptor endocytosis and retrovirus budding. *Genes Dev.* 18, 1737–1752.
- Babst, M., Wendland, B., Estepa, E.J., and Emr, S.D. (1998). The Vps4p AAA ATPase regulates membrane association of a Vps protein complex required for normal endosome function. *EMBO J.* 17, 2982–2993.
- Babst, M., Odorizzi, G., Estepa, E.J., and Emr, S.D. (2000). Mammalian tumor susceptibility gene 101 (TSG101) and the yeast homologue, Vps23p, both function in late endosomal trafficking. *Traffic* 1, 248–258.
- Babst, M., Katzmán, D.J., Estepa-Sabal, E.J., Meerloo, T., and Emr, S.D. (2002a). ESCRT-III: an endosome-associated heterooligomeric protein complex required for MVB sorting. *Dev. Cell* 3, 271–282.
- Babst, M., Katzmán, D.J., Snyder, W.B., Wendland, B., and Emr, S.D. (2002b). Endosome-associated complex, ESCRT-II, recruits transport machinery for protein sorting at the multivesicular body. *Dev. Cell* 3, 283–289.
- Bache, K.G., Brech, A., Mehlum, A., and Stenmark, H. (2003a). Hrs regulates multivesicular body formation via ESCRT recruitment to endosomes. *J. Cell Biol.* 162, 435–442.
- Bache, K.G., Raiborg, C., Mehlum, A., and Stenmark, H. (2003b). STAM and Hrs are subunits of a multivalent ubiquitin-binding complex on early endosomes. *J. Biol. Chem.* 278, 12513–12521.

- Bache, K.G., Slagsvold, T., Cabezas, A., Rosendal, K.R., Raiborg, C., and Stenmark, H. (2004). The growth-regulatory protein HCRP1/hVps37A is a subunit of mammalian ESCRT-I and mediates receptor down-regulation. *Mol. Biol. Cell* *15*, 4337–4346.
- Bilodeau, P.S., Winistorfer, S.C., Kearney, W.R., Robertson, A.D., and Piper, R.C. (2003). Vps27-Hse1 and ESCRT-I complexes cooperate to increase efficiency of sorting ubiquitinated proteins at the endosome. *J. Cell Biol.* *163*, 237–243.
- Bishop, N., and Woodman, P. (2001). TSG101/mammalian VPS23 and mammalian VPS28 interact directly and are recruited to VPS4-induced endosomes. *J. Biol. Chem.* *276*, 11735–11742.
- Bowers, K., and Stevens, T.H. (2005). Protein transport from the late Golgi to the vacuole in the yeast *Saccharomyces cerevisiae*. *Biochim. Biophys. Acta* *1744*, 438–454.
- Bowers, K., Lottridge, J., Helliwell, S.B., Goldthwaite, L.M., Luzio, J.P., and Stevens, T.H. (2004). Protein-protein interactions of ESCRT complexes in the yeast *Saccharomyces cerevisiae*. *Traffic* *5*, 194–210.
- Demirov, D.G., and Freed, E.O. (2004). Retrovirus budding. *Virus Res.* *106*, 87–102.
- Di Lello, P., Nguyen, B.D., Jones, T.N., Potempa, K., Kobor, M.S., Legault, P., and Omichinski, J.G. (2005). NMR structure of the amino-terminal domain from the Tfb1 subunit of TFIIF and characterization of its phosphoinositide and VP16 binding sites. *Biochemistry* *44*, 7678–7686.
- Doyotte, A., Russell, M.R., Hopkins, C.R., and Woodman, P.G. (2005). Depletion of TSG101 forms a mammalian “Class E” compartment: a multicisternal early endosome with multiple sorting defects. *J. Cell Sci.* *118*, 3003–3017.
- Eastman, S.W., Martin-Serrano, J., Chung, W., Zang, T., and Bieniasz, P.D. (2005). Identification of human VPS37C, a component of endosomal sorting complex required for transport-I important for viral budding. *J. Biol. Chem.* *280*, 628–636.
- Feng, G.H., Lih, C.J., and Cohen, S.N. (2000). TSG101 protein steady-state level is regulated posttranslationally by an evolutionarily conserved COOH-terminal sequence. *Cancer Res.* *60*, 1736–1741.
- Ferguson, K.M., Kavran, J.M., Sankaran, V.G., Fournier, E., Isakoff, S.J., Skolnik, E.Y., and Lemmon, M.A. (2000). Structural basis for discrimination of 3-phosphoinositides by pleckstrin homology domains. *Mol. Cell* *6*, 373–384.
- Fernandez-Borja, M., Wubbolts, R., Calafat, J., Janssen, H., Divecha, N., Dusseljee, S., and Neefjes, J. (1999). Multivesicular body morphogenesis requires phosphatidylinositol 3-kinase activity. *Curr. Biol.* *9*, 55–58.
- Futter, C.E., Collinson, L.M., Backer, J.M., and Hopkins, C.R. (2001). Human VPS34 is required for internal vesicle formation within multivesicular endosomes. *J. Cell Biol.* *155*, 1251–1264.
- Gillooly, D.J., Morrow, I.C., Lindsay, M., Gould, R., Bryant, N.J., Gullier, J.M., Parton, R.G., and Stenmark, H. (2000). Localization of phosphatidylinositol 3-phosphate in yeast and mammalian cells. *EMBO J.* *19*, 4577–4588.
- Goila-Gaur, R., Demirov, D.G., Orenstein, J.M., Ono, A., and Freed, E.O. (2003). Defects in human immunodeficiency virus budding and endosomal sorting induced by TSG101 overexpression. *J. Virol.* *77*, 6507–6519.
- Hicke, L., and Dunn, R. (2003). Regulation of membrane protein transport by ubiquitin and ubiquitin-binding proteins. *Annu. Rev. Cell Dev. Biol.* *19*, 141–172.
- Hierro, A., Sun, J., Rusnak, A.S., Kim, J., Prag, G., Emr, S.D., and Hurley, J.H. (2004). Structure of the ESCRT-II endosomal trafficking complex. *Nature* *431*, 221–225.
- Hurley, J.H., and Emr, S.D. (2006). The ESCRT complexes: Structure and mechanism of a membrane-trafficking network. *Annu. Rev. Biophys. Biomol. Struct.* *35*, 277–298.
- Hyvonen, M., Macias, M.J., Nilges, M., Oschkinat, H., Saraste, M., and Wilmanns, M. (1995). Structure of the binding site for inositol phosphates in a PH domain. *EMBO J.* *14*, 4676–4685.
- Johnson, M.C., Spidel, J.L., Ako-Adjei, D., Wills, J.W., and Vogt, V.M. (2005). The C-terminal half of TSG101 blocks Rous sarcoma virus budding and sequesters Gag into unique nonendosomal structures. *J. Virol.* *79*, 3775–3786.
- Katoh, K., Shibata, H., Suzuki, H., Nara, A., Ishidoh, K., Kominami, E., Yoshimori, T., and Maki, M. (2003). The ALG-2-interacting protein Alix associates with CHMP4b, a human homologue of yeast Snf7 that is involved in multivesicular body sorting. *J. Biol. Chem.* *278*, 39104–39113.
- Katzmann, D.J., Babst, M., and Emr, S.D. (2001). Ubiquitin-dependent sorting into the multivesicular body pathway requires the function of a conserved endosomal protein sorting complex, ESCRT-I. *Cell* *106*, 145–155.
- Katzmann, D.J., Odorizzi, G., and Emr, S.D. (2002). Receptor downregulation and multivesicular-body sorting. *Nat. Rev. Mol. Cell Biol.* *3*, 893–905.
- Katzmann, D.J., Stefan, C.J., Babst, M., and Emr, S.D. (2003). Vps27 recruits ESCRT machinery to endosomes during MVB sorting. *J. Cell Biol.* *162*, 413–423.
- Kim, J., Sitaraman, S., Hierro, A., Beach, B.M., Odorizzi, G., and Hurley, J.H. (2005). Structural basis for endosomal targeting by the Bro1 domain. *Dev. Cell* *8*, 937–947.
- Lemmon, M.A. (2005). Pleckstrin homology domains: two halves make a hole? *Cell* *120*, 574–576.
- Lietzke, S.E., Bose, S., Cronin, T., Klarlund, J., Chawla, A., Czech, M.P., and Lambright, D.G. (2000). Structural basis of 3-phosphoinositide recognition by pleckstrin homology domains. *Mol. Cell* *6*, 385–394.
- Lin, Y., Kimpler, L.A., Naismith, T.V., Lauer, J.M., and Hanson, P.I. (2005). Interaction of the mammalian endosomal sorting complex required for transport (ESCRT) III protein hSnf7-1 with itself, membranes, and the AAA+ ATPase SKD1. *J. Biol. Chem.* *280*, 12799–12809.
- Luhtala, N., and Odorizzi, G. (2004). Bro1 coordinates deubiquitination in the multivesicular body pathway by recruiting Doa4 to endosomes. *J. Cell Biol.* *166*, 717–729.
- Martin-Serrano, J., Yaravov, A., Perez-Caballero, D., and Bieniasz, P.D. (2003a). Divergent retroviral late-budding domains recruit vacuolar protein sorting factors by using alternative adaptor proteins. *Proc. Natl. Acad. Sci. USA* *100*, 12414–12419.
- Martin-Serrano, J., Zang, T., and Bieniasz, P.D. (2003b). Role of ESCRT-I in retroviral budding. *J. Virol.* *77*, 4794–4804.
- Meyer, H.H., Wang, Y., and Warren, G. (2002). Direct binding of ubiquitin conjugates by the mammalian p97 adaptor complexes, p47 and Ufd1-Npl4. *EMBO J.* *21*, 5645–5652.
- Morita, E., and Sundquist, W.I. (2004). Retrovirus budding. *Annu. Rev. Cell Dev. Biol.* *20*, 395–425.
- Odorizzi, G., Babst, M., and Emr, S.D. (1998). Fab1p PtdIns(3)P 5-kinase function essential for protein sorting in the multivesicular body. *Cell* *95*, 847–858.
- Peck, J.W., Bowden, E.T., and Burbelo, P.D. (2004). Structure and function of human Vps20 and Snf7 proteins. *Biochem. J.* *377*, 693–700.
- Pornillos, O., Higginson, D.S., Stray, K.M., Fisher, R.D., Garrus, J.E., Payne, M., He, G.-P., Wang, H.E., Morham, S.G., and Sundquist, W.I. (2003). HIV Gag mimics the Tsg101-recruiting activity of the human Hrs protein. *J. Cell Biol.* *162*, 425–434.
- Puertollano, R. (2005). Interactions of TOM1L1 with the multivesicular body sorting machinery. *J. Biol. Chem.* *280*, 9258–9264.
- Raiborg, C., Rusten, T.E., and Stenmark, H. (2003). Protein sorting into multivesicular endosomes. *Curr. Opin. Cell Biol.* *15*, 446–455.

- Raymond, C.K., Howald-Stevenson, I., Vater, C.A., and Stevens, T.H. (1992). Morphological classification of the yeast vacuolar protein sorting mutants: evidence for a prevacuolar compartment in class E vps mutants. *Mol. Biol. Cell* 3, 1389–1402.
- Rink, J., Ghigo, E., Kalaizidis, Y., and Zerial, M. (2005). Rab conversion as a mechanism of progression from early to late endosomes. *Cell* 122, 735–749.
- Schu, P.V., Takegawa, K., Fry, M.J., Stack, J.H., Waterfield, M.D., and Emr, S.D. (1993). Phosphatidylinositol 3-kinase encoded by yeast VPS34 gene essential for protein sorting. *Science* 260, 88–91.
- Scott, A., Chung, H.Y., Gonciarz-Swiatek, M., Hill, G.C., Whitby, F.G., Gaspar, J., Holton, J.M., Viswanathan, R., Ghaffarian, S., Hill, C.P., and Sundquist, W.I. (2005). Structural and mechanistic studies of VPS4 proteins. *EMBO J.* 24, 3658–3669.
- Shirk, A.J., Anderson, S.K., Hashemi, S.H., Chance, P.F., and Bennett, C.L. (2005). SIMPLE interacts with NEDD4 and TSG101: Evidence for a role in lysosomal sorting and implications for Charcot-Marie-Tooth disease. *J. Neurosci. Res.* 82, 43–50.
- Slagsvold, T., Aasland, R., Hirano, S., Bache, K.G., Raiborg, C., Trambaiolo, D., Wakatsuki, S., and Stenmark, H. (2005). Eap45 in mammalian ESCRT-II binds ubiquitin via a phosphoinositide-interacting GLUE domain. *J. Biol. Chem.* 280, 19600–19606.
- Strack, B., Calistri, A., Craig, S., Popova, E., and Gottlinger, H.G. (2003). AIP1/ALIX is a binding partner for HIV-1 p6 and EIAV p9 functioning in virus budding. *Cell* 114, 689–699.
- Stuchell, M.D., Garrus, J.E., Muller, B., Stray, K.M., Ghaffarian, S., McKinnon, R., Krausslich, H.-G., Morham, S.G., and Sundquist, W.I. (2004). The human endosomal sorting complex required for transport (ESCRT-I) and its role in HIV-1 budding. *J. Biol. Chem.* 279, 36059–36071.
- Sundquist, W.I., Schubert, H.L., Kelly, B.N., Hill, G.C., Holton, J.M., and Hill, C.P. (2004). Ubiquitin recognition by the human TSG101 protein. *Mol. Cell* 13, 783–789.
- Tan, S. (2001). A modular polycistronic expression system for overexpressing protein complexes in *Escherichia coli*. *Protein Expr. Purif.* 21, 224–234.
- Teo, H., Perisic, O., Gonzalez, B., and Williams, R.L. (2004a). ESCRT-II, an endosome-associated complex required for protein sorting; Crystal structure and interactions with ESCRT-III and membranes. *Dev. Cell* 7, 559–569.
- Teo, H., Veprintsev, D.B., and Williams, R.L. (2004b). Structural insights into endosomal sorting complex required for transport (ESCRT-I) recognition of ubiquitinated proteins. *J. Biol. Chem.* 279, 28689–28696.
- Thompson, B.J., Mathieu, J., Sung, H.H., Loeser, E., Rorth, P., and Cohen, S.M. (2005). Tumor suppressor properties of the ESCRT-II complex component Vps25 in *Drosophila*. *Dev. Cell* 9, 711–720.
- Vaccari, T., and Bilder, D. (2005). The *Drosophila* tumor suppressor vps25 prevents nonautonomous overproliferation by regulating notch trafficking. *Dev. Cell* 9, 687–698.
- von Schwedler, U.K., Stuchell, M., Muller, B., Ward, D.M., Chung, H.-Y., Morita, E., Wang, H.E., Davis, T., He, G.-P., Cimbora, D.M., et al. (2003). The protein network of HIV budding. *Cell* 114, 701–713.
- Whitley, P., Reaves, B.J., Hashimoto, M., Riley, A.M., Potter, B.V.L., and Holman, G.D. (2003). Identification of mammalian Vps24p as an effector of phosphatidylinositol 3,5-bisphosphate-dependent endosome compartmentalization. *J. Biol. Chem.* 278, 38786–38795.
- Yorikawa, C., Shibata, H., Waguri, S., Hatta, K., Horii, M., Katoh, K., Kobayashi, T., Uchiyama, Y., and Maki, M. (2005). Human CHMP6, a myristoylated ESCRT-III protein, interacts directly with an ESCRT-II component EAP20 and regulates endosomal cargo sorting. *Biochem. J.* 387, 17–26.
- Yu, J.W., Mendrola, J.M., Audhya, A., Singh, S., Keleti, D., DeWald, D.B., Murray, D., Emr, S.D., and Lemmon, M.A. (2004). Genome-wide analysis of membrane targeting by *S. cerevisiae* pleckstrin homology domains. *Mol. Cell* 13, 677–688.
- Zhou, H., and Zhou, Y. (2005). Fold recognition by combining sequence profiles derived from evolution and from depth-dependent structural alignment of fragments. *Proteins* 58, 321–328.

#### Accession Numbers

The coordinates for the ESCRT-I core and ESCRT-II GLUE domain structures described in this work have been deposited in the Protein Data Bank under ID code 2CAZ and 2CAY, respectively.

#### Note Added in Proof

The structure of the yeast ESCRT-I core was also independently determined by Kostelansky et al. (2006) in this issue of *Cell* (113–126).